# Odderon contribution in light of the LHC low-$t$ data

Emerson Luna

*Instituto de Física*

*Universidade Federal do Rio Grande do Sul*

*Diffraction and Low-x Physics*

Palermo, Italy, 2024

* in collaboration with V. A. Khoze and M. G. Ryskin

## Outline

- Brief introduction to Odderon
- Formalism: Pomeron and Odderon inputs
- The tension between the TOTEM and ALFA/ATLAS measurements
- Results
- Conclusions

# Introduction

■ The TOTEM publication of the measurements of the $\sigma_{tot}^{pp}$ and the $\rho^{pp}$ parameter at 13 TeV, prompted a renewal of interest in the potential existence of the high-energy *C*-odd (Odderon) contribution.

$\Rightarrow$ The observed value $\rho = (0.09 - 0.10) \pm 0.01$ turned out to be smaller than the predicted value ($\rho = 0.13 - 0.14$) based on Disp. Rel.

□ The new ATLAS/ALFA data recently confirmed this value of $\rho$

$\Rightarrow$ However, the value of $\sigma_{tot}^{pp}$ at 13 TeV reported by the ATLAS/ALFA team is approximately 5% lower than the average of values determined by TOTEM

## Introduction

■ The relatively small value of $\rho$ can be explained by the admixture of the $C$-odd amplitude, which survives at high LHC energies

$\Rightarrow$ Such amplitude with the intercept $\alpha_{Odd}$ close to 1 was predicted by the perturbative QCD

□ Another indication in favor of the Odderon emerged when the $d\sigma^{\bar{p}p}/dt$ data at $\sqrt{s} = 1.96$ TeV was compared with the corresponding $pp$ cross section (measured at 2.76 TeV but extrapolated to 1.96 TeV) in the diffractive dip region

$\Rightarrow$ A clear difference was observed

$\Rightarrow$ It is important to emphasize that this result depends on the specific extrapolation method between different energy levels

# Introduction

■ It should be noted that at very low $t$ close to zero and in the diffractive dip region, we deal with different $C$-odd contributions

$\Rightarrow$ To get a well-pronounced dip-bump structure near the dip in $d\sigma^{pp}/dt|_{2.76\,TeV}$ and rather flat behavior of $d\sigma^{\bar{p}p}/dt\big|_{1.96\,TeV}$, the real part of the Odderon $pp$ amplitude should be positive (in agreement with perturbative QCD expectation for the three gluon exchange)

$\Rightarrow$ On the other hand, to explain the low value of $\rho$ at $t = 0$, we need a negative Odderon real part

$\Rightarrow$ This negative real part could be induced by non-pert. effects

# Formalism

■ Our analysis is focused on differential cross-section data involving very small values of $t$

$\Rightarrow$ It requires consideration of the Coulomb-nuclear interference (CNI) region:

$$F^{C+N} = F^{N} + e^{i\alpha\phi(t)} F^{C}$$

□ We adopt

$$\phi(t) = \kappa \left[ \gamma + \ln\left(\frac{B|t|}{2}\right) + \ln\left(1 + \frac{8}{B\Lambda^2}\right) + \frac{4|t|}{\Lambda^2}\ln\left(\frac{\Lambda^2}{4|t|}\right) - \frac{2|t|}{\Lambda^2} \right]$$

where $\kappa$ flips sign when going from $pp$ ($\kappa = -1$) to $\bar{p}p$ ($\kappa = +1$)

## Formalism

$\Rightarrow$ $\Lambda^2$ is fixed at $0.71\ \mathrm{GeV}^2$

$\Rightarrow$ $B$ is the $t$ slope of elastic $d\sigma/dt \propto exp(Bt)$ cross-section

$\Rightarrow$ $\gamma = 0.577...$ is the Euler-Mascheroni constant

$\Rightarrow$ $\alpha$ is the electromagnetic coupling:

$$\alpha(q^2) = \frac{\alpha(0)}{1 - \frac{\alpha(0)}{3\pi} \ln\left(\frac{q^2+m_e^2}{m_e^2}\right)}$$

where $\alpha(0) \approx 1/137$

## Formalism

■ The Coulomb amplitude is expressed as

$$F^C = \kappa s \frac{2\alpha}{|t|} G^2(t)$$

where $G(t)$ is the electromagnetic form factor of the proton:

$$G(t) = \left[\frac{\Lambda^2}{\Lambda^2 + q^2}\right]^2$$

□ To account for the eikonalization, it is convenient to calculate the nuclear amplitude in terms of opacities:

$$\Omega_i(s,b) = \frac{2}{s}\int_0^\infty q\, dq\, J_0(bq)\, F_i^N(s,t)$$

where $i = \mathbb{P}, \mathbb{O}$ represent the Pomeron and Odderon exchanges

## Pomeron input

- The single Pomeron contribution is given by

$$F_{\mathbb{P}}^{N}(s,t) = \beta_{\mathbb{P}}^{2}(t)\,\eta_{\mathbb{P}}(t)\left(\frac{s}{s_0}\right)^{\alpha_{\mathbb{P}}(t)}$$

$\Rightarrow$ $\eta_{\mathbb{P}}(t) = -e^{-i\frac{\pi}{2}\alpha_{\mathbb{P}}(t)}$ is the even signature factor

$\Rightarrow$ $\beta_{\mathbb{P}}(t)$ is the elastic proton-Pomeron vertex

$\Rightarrow$ $\alpha_{\mathbb{P}}(t)$ is the Pomeron trajectory,

$$\alpha_{\mathbb{P}}(t) = 1 + \epsilon + \alpha'_{\mathbb{P}}t + \frac{m_\pi^2\beta_\pi^2}{32\pi^3}\,h(\tau)$$

where

$$h(\tau) = -\frac{4}{\tau}\,F_\pi^2(t)\left[2\tau - (1+\tau)^{3/2}\ln\left(\frac{\sqrt{1+\tau}+1}{\sqrt{1+\tau}-1}\right) + \ln\left(\frac{m^2}{m_\pi^2}\right)\right]$$

with $\epsilon > 0$, $\tau = 4m_\pi^2/|t|$, $m = 1$ GeV, and $m_\pi = 139.6$ MeV

## The Odderon input

■ From the standpoint of QCD (at the lowest order) the $C = +1$ amplitude arises from the exchange of two gluons and the $C = -1$ amplitude from the exchange of three gluons

■ Extensive theoretical studies have been directed towards uncovering corrections to these results, particularly in higher orders

□ In this scenario, the leading-log approximation allows for the summation of certain higher-order contributions to physical observables in high-energy particle scattering processes

$\Rightarrow$ This approach was widely used in the study of the QCD-Pomeron through the BFKL equation

## The Odderon input

$\Rightarrow$ In BFKL equation terms of the order $(\alpha_s \ln(s))^n$ are systematically summed at high energy (large $s$) and small strong coupling $\alpha_s$

$\Rightarrow$ The simplistic notion of bare two-gluon exchange gives way to the BFKL Pomeron, which, in an alternative representation, can be seen as the interaction of two reggeized gluons with one another

■ Beyond the BFKL Pomeron, the most elementary entity within perturbative QCD is the exchange involving three interacting reggeized gluons

□ The evolution of the three-gluon Odderon exchange as energy increases is governed by the BKP equation

$\Rightarrow$ A bound state solution of this Odderon equation was obtained with the intercept $\alpha_{\mathbb{O}}(0) = 1$

## The Odderon input

- Based on these QCD findings, we adopt in this work the simplest conceivable form for the Odderon trajectory:

$$\alpha_{\mathbb{O}}(t) = 1$$

- The Odderon contribution is given by

$$F^N_{\mathbb{O}}(s,t) = \beta^2_{\mathbb{O}}(t)\,\eta_{\mathbb{O}}(t)\left(\frac{s}{s_0}\right)^{\alpha_{\mathbb{O}}(t)}$$

$\Rightarrow$ $\eta_{\mathbb{O}}(t) = -ie^{-i\frac{\pi}{2}\alpha_{\mathbb{O}}(t)}$ is the odd signature factor

$\Rightarrow$ $\beta_{\mathbb{O}}(t)$ is the elastic proton-Odderon vertex

## $t$ dependence of the $\beta$ vertices

■ $\beta_{\mathbb{P}}(t)$ and $\beta_{\mathbb{O}}(t)$ are parameterized accounting for the observed deviation from a pure exponential behavior of the low-$|t|$ $d\sigma/dt$ data at LHC energies

$\Rightarrow$ Behavior identified by the TOTEM Collaboration

□ The TOTEM group has extended the pure exponential to a cumulant expansion,

$$\frac{d\sigma}{dt}(t) = \left.\frac{d\sigma}{dt}\right|_{t=0} \exp\left(\sum_{n=1}^{N_b} b_n t^n\right)$$

where the optimal fit was achieved for $N_b = 3$, yielding $\chi^2/DoF = 1.22$ and a corresponding $p$-value of 8.0%

# $t$ dependence of the $\beta$ vertices

■ Based on this result, we have written the Pomeron- and Odderon-proton vertices as

$$\beta_{\mathbb{P}}(t) = \beta_{\mathbb{P}}(0)e^{\left(At+Bt^2+Ct^3\right)/2}$$

and

$$\beta_{\mathbb{O}}(t) = \beta_{\mathbb{O}}(0)e^{Dt/2}$$

respectively

## Models

■ We allow for the low mass diffractive dissociation (Good-Walker formalism)

$\Rightarrow$ The Pomeron and Odderon couplings to the two diffractive states $|\phi_k\rangle$ are

$$\beta_{i,k}(t) = (1 \pm \gamma)\beta_i(t)$$

with $i = \mathbb{P}$ or $\mathbb{O}$, and $\gamma = 0.55$

□ The eikonalized amplitude in $(s,t)$-space is then given by

$$\begin{aligned}\mathcal{A}(s,t) &= is \int_0^\infty b\, db\, J_0(bq) \left[1 - \frac{1}{4}\, e^{i(1+\gamma)^2\Omega(s,b)/2}\right. \\ &\quad \left. -\frac{1}{2}\, e^{i(1-\gamma^2)\Omega(s,b)/2} - \frac{1}{4}\, e^{i(1-\gamma)^2\Omega(s,b)/2}\right]\end{aligned}$$

where $\Omega(s,b)$ is the total opacity

# Models

■ We consider two versions for the total opacity with different signs for the Odderon contribution

□ In the first version, referred to as ‘Model **I**’, we have

$$\Omega(s, b) = \Omega_{\mathbb{P}}(s, b) \mp \Omega_{\mathbb{O}}(s, b)$$

□ In the second version, called ‘Model **II**’, we have

$$\Omega(s, b) = \Omega_{\mathbb{P}}(s, b) \pm \Omega_{\mathbb{O}}(s, b)$$

$\Rightarrow$ In both cases the upper sign is for $pp$ and the lower sign is for $\bar{p}p$

## Models

- The total cross section and the $\rho$ parameter are expressed in terms of the nuclear eikonalized amplitude $\mathcal{A}(s,t)$:

$$\sigma_{tot}(s) = \frac{4\pi}{s} \mathrm{Im}\, \mathcal{A}(s, t = 0)$$

$$\rho(s) = \frac{\mathrm{Re}\, \mathcal{A}(s, t = 0)}{\mathrm{Im}\, \mathcal{A}(s, t = 0)}$$

- The full scattering amplitude is written as

$$F^{C+N}(s,t) = \mathcal{A}(s,t) + e^{i\alpha\phi(t)} F^{C}(s,t)$$

## Models

- Finally, the differential and the total elastic cross sections are given by

$$\frac{d\sigma}{dt}(s,t) = \frac{\pi}{s^2}\left|\mathcal{A}(s,t) + e^{i\alpha\phi}\mathcal{F}^C(s,t)\right|^2$$

and

$$\sigma_{el}(s) = \frac{\pi}{s^2}\int_{-\infty}^{0} dt\,|\mathcal{A}(s,t)|^2$$

# Results

■ The LHC has released exceptionally precise measurements of diffractive processes

□ These measurements, particularly the total and differential cross sections obtained from ATLAS and TOTEM Collaborations, enable us to determine the Pomeron and Odderon parameters accurately

$\Rightarrow$ However, these experimental results unveil a noteworthy tension between the TOTEM and ATLAS measurements

$\Rightarrow$ For instance, when comparing the TOTEM and the ATLAS result for $\sigma_{tot}^{pp}$ at $\sqrt{s} = 8$ TeV, the discrepancy between the values corresponds to 2.6 $\sigma$

## Results

■ In order to systematically explore the tension between TOTEM and ATLAS results, we perform global fits to $pp$ and $\bar{p}p$ differential cross-section data while considering three distinct datasets:

**Ensemble A**: $\frac{d\sigma^{\bar{p}p,pp}}{dt}\Big|_{\text{CERN-ISR}} + \frac{d\sigma^{\bar{p}p}}{dt}\Big|_{S\bar{p}pS} + \frac{d\sigma^{\bar{p}p}}{dt}\Big|_{\text{Tevatron}} + \frac{d\sigma^{pp}}{dt}\Big|_{\text{ATLAS/ALFA}}$

**Ensemble T**: $\frac{d\sigma^{\bar{p}p,pp}}{dt}\Big|_{\text{CERN-ISR}} + \frac{d\sigma^{\bar{p}p}}{dt}\Big|_{S\bar{p}pS} + \frac{d\sigma^{\bar{p}p}}{dt}\Big|_{\text{Tevatron}} + \frac{d\sigma^{pp}}{dt}\Big|_{\text{TOTEM}}$

**Ensemble A⊕T**: $\frac{d\sigma^{\bar{p}p,pp}}{dt}\Big|_{\text{CERN-ISR}} + \frac{d\sigma^{\bar{p}p}}{dt}\Big|_{S\bar{p}pS} + \frac{d\sigma^{\bar{p}p}}{dt}\Big|_{\text{Tevatron}} + \frac{d\sigma^{pp}}{dt}\Big|_{\text{ATLAS/ALFA}} + \frac{d\sigma^{pp}}{dt}\Big|_{\text{TOTEM}}$

$\Rightarrow$ We carry out global fits to the two distinct ensembles using a $\chi^2$ fitting procedure, where $\chi^2_{min}$ follows a $\chi^2$ distribution with $\nu$ DoF

$\Rightarrow$ We adopt an interval $\chi^2 - \chi^2_{min}$ corresponding to a 90% confidence level (CL).

# Results

■ Since the absolute values of cross sections measured at the same energy by different groups do not agree, we have introduced normalization factors $N_i$ for high-energy $d\sigma/dt$ data

$\Rightarrow$ $i = 7[A]$, $8[A]$, and $13[A]$ for the ATLAS/ALFA data and $i = 7[T]$, $8[T]$, and $13[T]$ for the TOTEM data (here the numbers within the indices $i$ correspond to the values of $\sqrt{s}$)

$\Rightarrow$ Analogous normalization factors are introduced for the Tevatron data with $i = 1.8[E]$ and $i = 1.8[C]$, i.e. $N_{1.8[E]}$ for the E710 data and $N_{1.8[C]}$ for the CDF data

$\Rightarrow$ Despite being the only data set measured at $\sqrt{s} = 546$ GeV, we also included a normalization factor for $d\sigma^{\bar{p}p}/dt\big|_{\sqrt{s}=546\,\mathrm{GeV}}$, namely $N_{546}$

## Results

■ Furthermore, when dealing with the data sets incorporating normalization factors $N_i$, we make use of the formula

$$\chi^2 = \sum_{ij} \frac{(N_i ds_{ij}^{th} - ds_{ij}^{exp})^2}{(\delta_{ij}^{rem})^2} + \sum_i \frac{(1 - N_i)^2}{\delta_i^2}$$

⇒ $i$ denotes the particular set of data while $j$ denotes the point $t_j$ in this set of data

⇒ $ds^{th}$ is the theoretically calculated $d\sigma/dt$ cross section while $ds^{exp}$ is the value measured at the same $ij$ point experimentally

⇒ $\delta_i$ is the normalization uncertainty of the given ($i$) set of data and $\delta_{ij}^{rem}$ is the remaining error at the point $ij$ calculated as
$(\delta_{ij}^{rem})^2 = \delta_{tot,ij}^2 - \delta_i^2$

⇒ As a rule the value of $\delta^{rem}$ is dominantly the statistical error

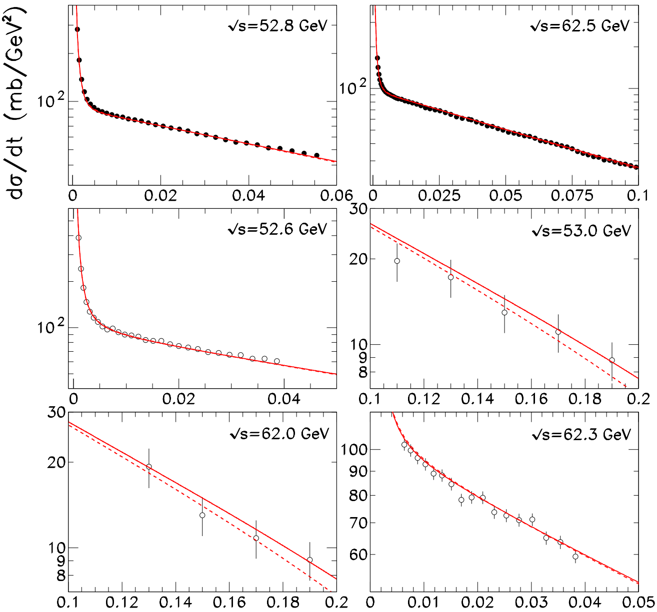


FIG.1. Description of the $t$ dependence of the elastic *pp*- and $\bar{p}p$-cross sections measured at CERN-ISR. The dashed and solid curves depict the results obtained using Models I and II, respectively

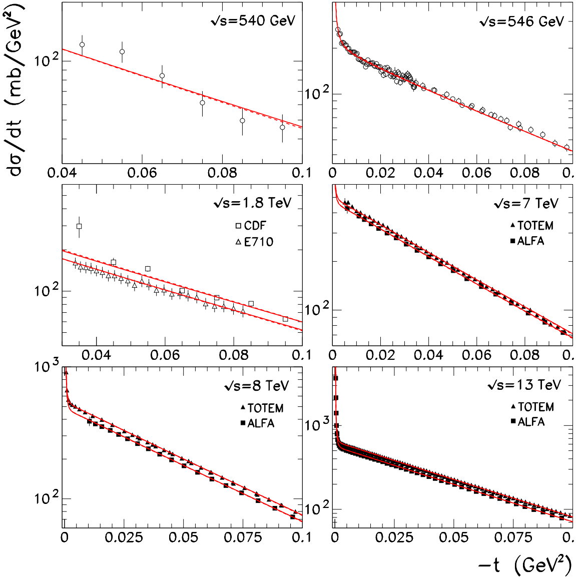


FIG.2. Description of the $t$ dependence of the elastic $pp$- and $\bar{p}p$-cross sections measured at the $S\bar{p}pS$, the Tevatron and the LHC colliders. The dashed and solid curves depict the results obtained using Models I and II, respectively. The lower curves describe the ATLAS/ALFA (E710) data while the upper curves correspond to the TOTEM (CDF) data; in both cases, the normalization factors $N_i$ are accounted for

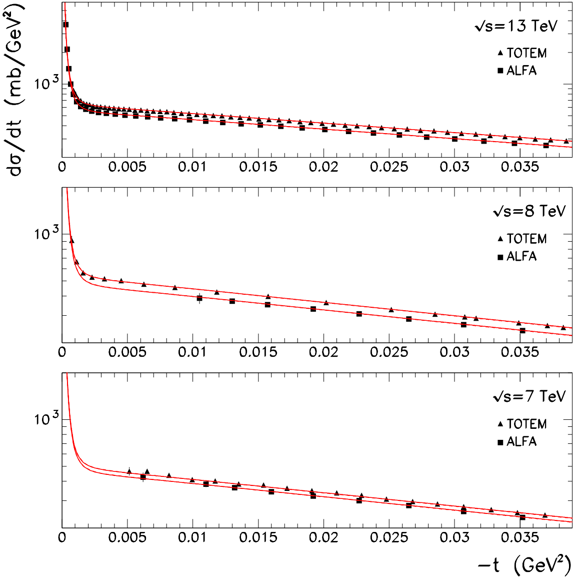


FIG.3. The same as Fig. 2 but for the CNI region where the Odderon contribution reveals itself

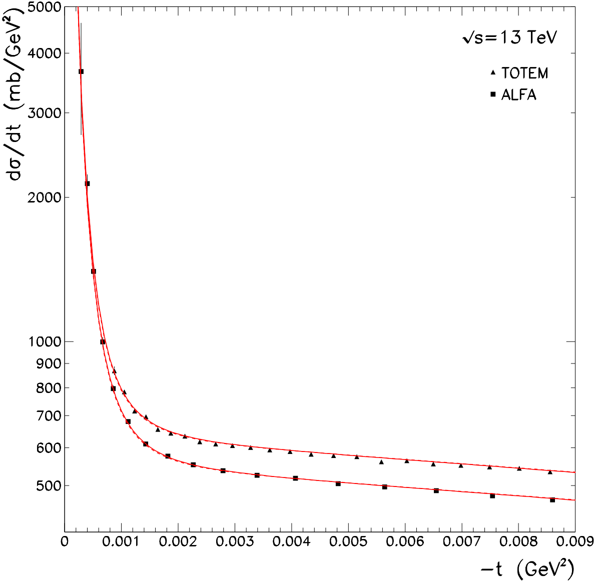


FIG.4. The same as Figs. 2 and 3 but in another scale to better see the quality of precise 13 TeV data description

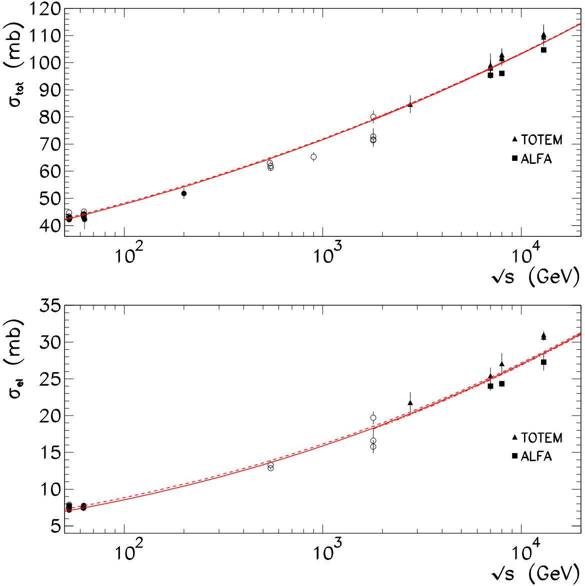


FIG.5. Description of the total and elastic $pp$ (●, ▲, ■) and $\bar{p}p$ (○) cross sections. The dotted and dashed-dotted curves represent the results for $pp$ and $\bar{p}p$ channels, respectively, obtained from the global fit to Ensemble A $\oplus$ T using Model I. These curves are indistinguishable. The solid and dashed curves represent the results for $pp$ and $\bar{p}p$ channels, respectively, obtained from the global fit to Ensemble A $\oplus$ T using Model II

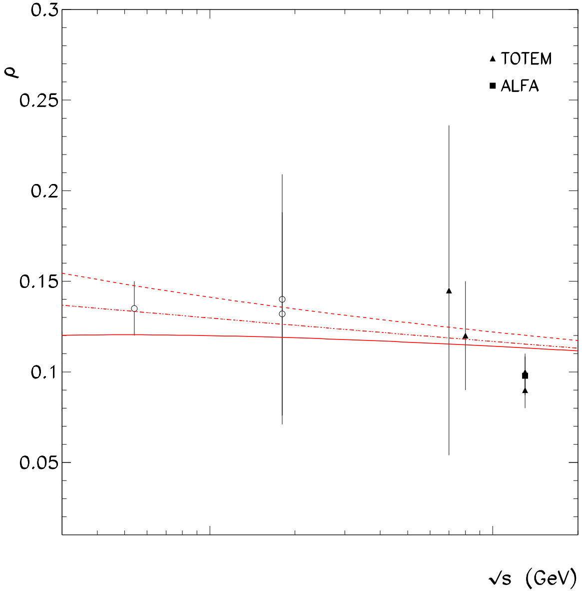


FIG.6. $\rho$ parameter for $pp$ (▲, ■) and $\bar{p}p$ (○) elastic amplitude. The dotted and dashed-dotted curves represent the results for $\rho^{pp}$ and $\rho^{\bar{p}p}$, respectively, obtained from the global fit to Ensemble A $\oplus$ T using the Model I. These curves are indistinguishable. The solid and dashed curves represent the results for $\rho^{pp}$ and $\rho^{\bar{p}p}$, respectively, obtained from the global fit to Ensemble A $\oplus$ T using the Model II

**Table:** Values of the parameters obtained in the global fits to Ensemble $A \oplus T$.

| | **Model I** | **Model II** | **Model II** |
|---|---|---|---|
| $\beta_{\mathbb{P}}(0)$ | 2.247±0.013 | 2.259±0.016 | 2.307±0.022 |
| $\epsilon$ | 0.1173±0.0021 | 0.1180±0.0020 | 0.1134±0.0019 |
| $\alpha'_{P}$ (GeV$^{-2}$) | 0.124±0.024 | 0.128±0.022 | 0.133±0.023 |
| $A$ (GeV$^{-2}$) | 5.01±0.20 | 4.78±0.21 | 4.72±0.21 |
| $B$ (GeV$^{-4}$) | 6.61±0.99 | 6.7±1.1 | 6.9±1.2 |
| $C$ (GeV$^{-6}$) | 20.4±5.7 | 17.7±4.0 | 17.0±4.2 |
| $\beta_{\mathbb{O}}(0)$ | $(0.15\times10^{-4})\pm39$ | 0.90±0.18 | 0.88±0.18 |
| $N_{546}$ | 0.941 | 0.933 | 0.958 |
| $N_{1.8[E]}$ | 0.923 | 0.912 | 0.944 |
| $N_{1.8[C]}$ | 1.087 | 1.070 | 1.109 |
| $N_{7[A]}$ | 1.015 | 1.015 | 1.056 |
| $N_{8[A]}$ | 1.003 | 1.003 | 1.045 |
| $N_{13[A]}$ | 1.009 | 1.009 | 1.052 |
| $N_{7[T]}$ | 1.077 | 1.077 | 1.121 |
| $N_{8[T]}$ | 1.121 | 1.121 | 1.167 |
| $N_{13[T]}$ | 1.150 | 1.150 | 1.200 |
| $\rho^{pp}(\sqrt{s}=13$ TeV) | 0.114 | 0.111 | 0.109 |
| $\rho^{\bar{p}p}(\sqrt{s}=13$ TeV) | 0.114 | 0.119 | 0.116 |
| Allowed $N_i$ interval | [0.85,1.15] | [0.85,1.15] | [0.80,1.20] |
| $\nu$ | 504 | 504 | 504 |
| $\chi^2/\nu$ | 1.44 | 1.11 | 1.03 |

**Table:** Predictions for $\sigma_{tot}^{\bar{p}p,pp}$, $\sigma_{el}^{\bar{p}p,pp}$, and $\rho^{\bar{p}p,pp}$ using Models I and II. These results were derived for the scenario with $D = A/2$

| | Model I | | | Model II | | |
|---|---|---|---|---|---|---|
| $\sqrt{s}$ (TeV) | $\sigma_{tot}^{pp}$ \| $\sigma_{tot}^{\bar{p}p}$ (mb) | $\sigma_{el}^{pp}$ \| $\sigma_{el}^{\bar{p}p}$ (mb) | $\rho^{pp}$ \| $\rho^{\bar{p}p}$ | $\sigma_{tot}^{pp}$ \| $\sigma_{tot}^{\bar{p}p}$ (mb) | $\sigma_{el}^{pp}$ \| $\sigma_{el}^{\bar{p}p}$ (mb) | $\rho^{pp}$ \| $\rho^{\bar{p}p}$ |
| 0.541 | 64.2 \| 64.2 | 13.2 \| 13.2 | 0.130 \| 0.130 | 63.8 \| 64.1 | 13.3 \| 13.5 | 0.117 \| 0.144 |
| 1.8 | 78.0 \| 78.0 | 17.6 \| 17.6 | 0.124 \| 0.124 | 77.6 \| 77.8 | 17.7 \| 17.9 | 0.116 \| 0.133 |
| 7 | 95.9 \| 95.9 | 23.9 \| 23.9 | 0.117 \| 0.117 | 95.7 \| 95.9 | 24.0 \| 24.2 | 0.113 \| 0.123 |
| 8 | 97.9 \| 97.9 | 24.5 \| 24.5 | 0.116 \| 0.116 | 97.6 \| 97.8 | 24.7 \| 24.8 | 0.113 \| 0.122 |
| 13 | 105.1 \| 105.1 | 27.2 \| 27.2 | 0.114 \| 0.114 | 104.9 \| 105.1 | 27.3 \| 27.4 | 0.111 \| 0.119 |

## **Table:** Results using Model II

| | | | | | |
|---|---|---|---|---|---|
| | | | Ensemble $A$ | | |
| $D$ (GeV$^{-2}$) | $0.1A$ | $0.3A$ | $0.5A$ | $0.7A$ | $0.9A$ |
| $\beta_{\mathbb{O}}(0)$ | 0.93±0.22 | 0.85±0.22 | 0.80±0.21 | 0.77±0.19 | 0.74±0.18 |
| $\beta_{\mathbb{P}}(0)$ | 2.370±0.035 | 2.384±0.036 | 2.386±0.037 | 2.386±0.040 | 2.388±0.039 |
| $\nu$ | 332 | 332 | 332 | 332 | 332 |
| $\chi^2/\nu$ | 0.96 | 0.97 | 0.97 | 0.97 | 0.96 |
| $\rho^{pp}(\sqrt{s} = 13$ TeV) | 0.105 | 0.105 | 0.105 | 0.104 | 0.104 |
| $\rho^{\bar{p}p}(\sqrt{s} = 13$ TeV) | 0.113 | 0.112 | 0.113 | 0.114 | 0.114 |
| $\sigma_{tot}^{pp}(\sqrt{s} = 13$ TeV) (mb) | 98.0 | 98.0 | 98.0 | 98.0 | 98.0 |
| $\sigma_{tot}^{pp}(\sqrt{s} = 13$ TeV) (mb) | 98.2 | 98.2 | 98.2 | 98.2 | 98.1 |
| | | | Ensemble $T$ | | |
| $D$ (GeV$^{-2}$) | $0.1A$ | $0.3A$ | $0.5A$ | $0.7A$ | $0.9A$ |
| $\beta_{\mathbb{O}}(0)$ | 1.09±0.22 | 0.96±0.18 | 0.90±0.16 | 0.86±0.15 | 0.83±0.14 |
| $\beta_{\mathbb{P}}(0)$ | 2.236±0.022 | 2.258±0.016 | 2.260±0.016 | 2.260±0.017 | 2.259±0.018 |
| $\nu$ | 418 | 418 | 418 | 418 | 418 |
| $\chi^2/\nu$ | 1.28 | 1.30 | 1.29 | 1.28 | 1.27 |
| $\rho^{pp}(\sqrt{s} = 13$ TeV) | 0.112 | 0.112 | 0.111 | 0.111 | 0.110 |
| $\rho^{\bar{p}p}(\sqrt{s} = 13$ TeV) | 0.119 | 0.118 | 0.119 | 0.119 | 0.120 |
| $\sigma_{tot}^{pp}(\sqrt{s} = 13$ TeV) (mb) | 104.9 | 104.9 | 104.9 | 104.9 | 104.9 |
| $\sigma_{tot}^{pp}(\sqrt{s} = 13$ TeV) (mb) | 105.1 | 105.1 | 105.1 | 105.1 | 105.1 |
| | | | Ensemble $A \oplus T$ | | |
| $D$ (GeV$^{-2}$) | $0.1A$ | $0.3A$ | $0.5A$ | $0.7A$ | $0.9A$ |
| $\beta_{\mathbb{O}}(0)$ | 1.09±0.24 | 0.95±0.19 | 0.90±0.18 | 0.86±0.17 | 0.83±0.16 |
| $\beta_{\mathbb{P}}(0)$ | 2.235±0.023 | 2.257±0.016 | 2.259±0.016 | 2.258±0.016 | 2.258±0.017 |
| $\nu$ | 504 | 504 | 504 | 504 | 504 |
| $\chi^2/\nu$ | 1.11 | 1.12 | 1.11 | 1.10 | 1.09 |
| $\rho^{pp}(\sqrt{s} = 13$ TeV) | 0.112 | 0.112 | 0.111 | 0.111 | 0.110 |
| $\rho^{\bar{p}p}(\sqrt{s} = 13$ TeV) | 0.119 | 0.118 | 0.119 | 0.119 | 0.120 |
| $\sigma_{tot}^{pp}(\sqrt{s} = 13$ TeV) (mb) | 104.9 | 104.9 | 104.9 | 104.9 | 104.9 |
| $\sigma_{tot}^{pp}(\sqrt{s} = 13$ TeV) (mb) | 105.1 | 105.1 | 105.1 | 105.1 | 105.1 |

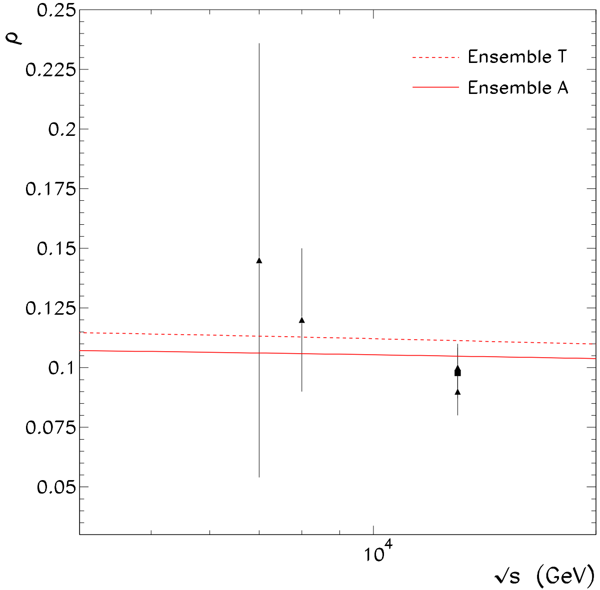


FIG.7. Description of $\rho$ parameter for *pp* elastic amplitude measured by TOTEM (▲) and ATLAS/ALFA (■) Collaborations. The dashed (solid) curve represents the predicted $\rho^{pp}$ from the global fit using Ensemble T (Ensemble A)

## Conclusions

■ The differential $pp$ and $\bar{p}p$ cross sections $d\sigma/dt$ at low $|t| < 0.1$ GeV$^2$ and collider energies (from $\sqrt{s} > 50$ GeV to 13 TeV) are successfully described ($\chi^2/\nu = 1.11$) within the two-channel eikonal model

□ To avoid the double counting we do not include in the fit the $\sigma_{tot}$ and $\rho$ data (which were obtained from the description of the same $d\sigma/dt$ data points)

■ The model accounts for the screening of the Odderon contribution by the Pomerons including the $C$-even (Pomeron) and $C$-odd (Odderon) multiple exchanges

■ To resolve the discrepancy between the TOTEM and ATLAS/ALFA (CDF and E710 in the Tevatron case) data we introduce the normalization coefficients, $N_i$ writing the theoretical prediction as $d\sigma^{exp}/dt = N_i d\sigma^{Th}/dt$

## Conclusions

■ We show that the presence of *C*-odd (Odderon) contribution essentially improves the fit; however it does not noticeably change the predicted value of $\rho^{pp}$ at 13 TeV

■ The main lessons about the Odderon coming from this study are:

$\Longrightarrow$ The description using the Odderon improves the fit (the $\chi^2/\nu$ is the lowest one)

$\Longrightarrow$ The sign of the Odderon amplitude needed to describe the very low $|t|$ data is opposite to that predicted by the perturbative QCD three-gluon exchange contribution

## Conclusions

$\Longrightarrow$ The quality of the description weakly depends on the Odderon $t$-slope, $D$, (leading to practically the same values of $\sigma_{tot}$ and $\rho$). However, for smaller $D$ we need larger coupling $\beta_{\mathbb{O}}$ to compensate for a stronger absorption caused by the Pomeron screening at small impact parameters $b$

$\Longrightarrow$ The Odderon-proton coupling, $\beta_{\mathbb{O}}$, is smaller than that for the Pomeron, $\beta_{\mathbb{P}}$. For $D = A/2$ we get $\beta_{\mathbb{O}}/\beta_{\mathbb{P}} = 0.40$, however after accounting for screening by the Pomeron the final $C$-odd contribution to $\rho$ at 13 TeV becomes quite small, $\delta\rho = (\rho^{\bar{p}p} - \rho^{pp})/2 \leq 0.004$ (see Table 1) and it will be challenging to enlarge it. Otherwise, we will get too large $\rho^{\bar{p}p}$ at $\sqrt{s} \sim 541$ GeV in disagreement with the data

THANK YOU

## Resumations in QCD

■ Every physical observable can be written, in pQCD, as a power series in $\alpha_s$

$\Longrightarrow$ in these series the coupling constant is accompanied by large logarithms, which need to be resummed

$\Longrightarrow$ according to the type and to the powers of logarithms that are effectively resummed one gets different evolution equations

■ The solution of the DGLAP equation sums over all orders in $\alpha_s$ the contributions from leading, single, collinear logarithms of the form $\alpha_s \ln\left(Q^2/Q_0^2\right)$

$\Longrightarrow$ it does not include leading, single, soft singularities of the form $\alpha_s \ln\left(1/x\right)$, which are treated instead by the BFKL equation

■ The BFKL equation describes the $x$-evolution of PDFs at fixed $Q^2$

## Resummations in QCD

■ The phase space regions which contribute these logarithms enhancements are associated with configurations in which successive partons have strongly ordered transverse, $k_T$, or longitudinal, $k_L \equiv x$, momenta:

$\Rightarrow \alpha_s L_Q \sim 1$, $\alpha_s L_x \ll 1$: $Q^2 \gg k_{T,n}^2 \gg \cdots \gg k_{T,1}^2 \gg Q_0^2$

$\Rightarrow \alpha_s L_x \sim 1$, $\alpha_s L_Q \ll 1$: $x \ll x_n \ll \cdots \ll x_1 \ll x_0$

■ At small-$x$ and slow $Q^2$ (where gluons are dominant) we do not have strongly ordered $k_T$

$\Rightarrow$ we have to integrate over the full range of $k_T$

$\Rightarrow$ this leads us to work with the *unintegrated* gluon PDF $\tilde{g}(x, k_T^2)$:

$$xg(x, Q^2) = \int^{Q^2} \frac{dk_T^2}{k_T^2} \tilde{g}(x, k_T^2)$$

## Positivity

■ The phase factor is associated with the positivity property

$\Rightarrow$ However, unlike Pomeron, the Odderon is not constrained by positivity requirements

$\Rightarrow$ From a theoretical standpoint, this implies that it is not possible to determine the phase of the Odderon mathematically

□ This issue can be succinctly grasped: in the forward direction the physical amplitudes $\mathcal{F}^{pp}_{\bar{p}p}(s)$ can be written as $\mathcal{F}^{pp}_{\bar{p}p}(s) = F^{+}(s) \pm F^{-}(s)$

□ Considering that the only relevant contributions are those arising from the Pomeron and the Odderon exchanges, we can write the symmetric and antisymmetric amplitudes as $F^{+}(s) = R_{\mathbb{P}}(s) + iI_{\mathbb{P}}(s)$ and $F^{-}(s) = R_{\mathbb{O}}(s) + iI_{\mathbb{O}}(s)$

□ From the optical theorem, we have $s\sigma_{tot}^{pp,\bar{p}p}(s) = 4\pi \, \mathrm{Im}\, \mathcal{F}_{\bar{p}p}^{pp}(s) > 0$, which implies that

$$\mathrm{Im}\, \mathcal{F}_{\bar{p}p}^{pp}(s) = I_{\mathbb{P}}(s) \pm I_{\mathbb{O}}(s) > 0$$

and, in turn,

$$I_{\mathbb{P}}(s) > |I_{\mathbb{O}}(s)|$$

As a consequence,

$$I_{\mathbb{P}}(s) = \frac{s}{2}\left[\sigma_{tot}^{pp}(s) + \sigma_{tot}^{\bar{p}p}(s)\right] > 0$$

while

$$I_{\mathbb{O}}(s) = \frac{s}{2}\left[\sigma_{tot}^{pp}(s) - \sigma_{tot}^{\bar{p}p}(s)\right]$$

is not bound by the same positivity requirements